Email: editor@ijerst.com or editor.ijerst@gmail.com

International Journal of Engineering Research and Science & Technology

ISSN 2319-5991 www.ijerst.com

Vol. 21, Issue 2, 2025

Stability Analysis Of Grid Forming Power Control For Reliable Energy Systems

[1]B. Rambabu, [2]Kamarathi Kalyan Kumar, [3]Edralla Mahesh, [4]Obulappagari Durga,
[5]Kuruba Swathi, [6]Butta Ganesh,
[1]Assistant Professor, Department Of EEE, Ananthalakshmi Institute Of Technology And Sciences, Itikalapalli, Near Sk University,Ananthapur.
[2,3,4,5,6]Student, Department Of EEE, Ananthalakshmi Institute Of Technology And Sciences, Itikalapalli, Near Sk University,Ananthapur.

ABSTRACT

In an effort to achieve stable system functioning, grid-forming inverters (GFMs) are being introduced, which are similar to synchronous generators (SGs). Paradoxically, in high short circuit ratio (SCR) situations, GFMs have unstable output characteristics, despite their intended replacement of conventional grid-following inverters (GFLs)—which introduces system inertia and considerably adds to fault current. Implementing a mathematical plant model of the fundamental GFM structure and integrating grid-connected GFM and the system's SCR for grid dynamics maintenance are both covered in this study. To achieve this goal, we provide a SIMO model of an APC-enabled GFM for use in assessing the stability of the grid during intermittent power outages, as well as a system frequency response model that takes into account the dynamic performance of both the SG and the GFM. It was also set up so that APC could mimic big grid events. An existing APC approach, such as droop or virtual synchronous machine (VSM), is compared to the proposed APC's performance in terms of step response and frequency response characteristics. Stable operation may be anticipated by actively assembling the controller during the SCR, which continually changes in both small and big grid events, according to simulation findings obtained using MATLAB and PSS/e. Terms of Index Grid-forming inverters (GFIs), active power control (APC), SIO modeling, droop, short circuit ratio (SCR), system frequency response (SFR), and virtual synchronous machines (VSMs) are all terms related to grid-forming inverters.

INTRODUCTION

Alterations to the renewable energy supply chain are becoming more common. Current synchronous generators (SGs) are being supplanted by renewable energy sources that rely on power electronic technology. We currently rely on renewable energy sources—also known as inverter-based resources (IBRs)—to provide a large amount of our electrical needs. These sources include wind turbines, solar photovoltaics (PV), and energy storage systems (ESS). Meng Huang was the assistant editor who oversaw the manuscript's evaluation and gave final approval for publishing. 112626 At now, interconnected power-relay bridges (IBRs) only inject power into the system by observing the voltage at the point of common coupling (PCC) and its amplitude, phase angle, and frequency. The control structure of the majority of IBRs is known as grid-following inverters (GFLs). Here are some issues that have come up as the integration of GFL-based IBR resources has grown. Addressing stability issues in phase-locked loop (PLL) dynamics at low short circuit ratio (SCR) and grid transient instability, which leads to fault currents, has been done [1], [2]. Physical inertial energy constraint reduces system inertia, which in turn reduces frequency stability. As a method that may help improve the transient stability and inertial resources of the system, the grid-forming inverter (GFM) has recently gained interest in this regard [3, 4]. In contrast to the GFL, which acts as a source of current, the GFM mimics the SG by acting as a voltage source and controlling the phase angle itself. Many GFM control approaches have been suggested to increase system resilience since GFM's recent inception, and it has been extensively incorporated into system operation. The simplest linear control system was developed using droop control as a foundational approach [5, 6]. You can

International Journal of Engineering Research and Science & Technology

ISSN 2319-5991 www.ijerst.com

Vol. 21, Issue 2, 2025

regulate the frequency and voltage using its SG properties, which are P → f and Q → V. In the context of virtual synchronous machines (VSMs), studies on power loops have been carried out, simulating the GFM swing equation [7], [8]. A capacitor's dynamic reaction is mirrored by matching control. It produces a phase angle by taking the DC current into account, and it is comparable to the SG swing equation [9]. Virtual oscillator control (VOC) is a nonlinear oscillator that incorporates dead zone and Van der Pol oscillators [10], [11], breaking away from earlier machine-based controllers. The active power control (APC) schemes include a variety of GFM control methods, and they have shown a number of benefits to the system's dynamic performance in disturbance situations and fault current contributions. Nevertheless, GFM may encounter difficulties in situations with significant SCR, which might result in voltage and frequency regulation instability [12], [13]. Therefore, in order to stabilize grid formation capabilities under these situations, advanced control procedures are necessary. Research on the correlation between system SCR and GFM has shown that GFM self-synchronization is more and more unstable with increasing SCR [14], [15]. A little phase mismatch between the GFM and the system causes substantial active power changes as the SCR grows [16]. An examination of the frequency response properties taking into account several GFM APC controls was offered inside the framework of a load increase, and an issue that may differ depending on control circumstances, such parameter setting, was discovered [17], [18]. Mathematical model-based plant stability research has examined IBR resource stability, which could be problematic for systems experiencing tiny grid events. It was from an LC filter that the SISO transfer function was developed [19], [20]. A capacitor with an additional dampening resistor was used to address the resonance issue caused by inverter filters [21], [22]. Because the filter-configured GFM generates voltage, studying the plant model that does the same is essential. In addition, a plant model was constructed to study the association between impedance and control-loop gain [23]. A relational expression was proposed between the voltage-controlled plant model and the system SCR via the inverter equivalent impedance, providing a foundation for stability analysis [24]. Lastly, the GFM plant model and the APC, which incorporates the GFM's real active power output, must be combined in order to examine the stability of the active power. What follows is an attempt to combine the APC with the plant model for SISO. Decoupling the active and reactive powers allowed for the investigation of a small-signal model [25], [26], and the presentation of a parametric design [27] based on that research. Researchers looked at how grid-connected inverters maintained a constant active power angle [28]. A stability study for the phase margin was carried out after obtaining the GFM APC's transfer function [18]. In order to construct the APC with a second-order voltage transfer function, a voltage plant model was used as an approximation [29]. No matter the SCR, a stable margin may be created using a strong parametric tuning architecture for droop and VSM [30]. The APC settings and SCR were used in a sensitivity analysis [31]. It is possible for the GFM to diverge in big grid events even when the APC controller is set up to take stability and SCR into account in minor grid events [16], [17]. It is necessary to investigate other approaches to ensuring the steady power output of GFMinbig grid events, as stability analysis is often reserved for SFRs [32] and not the SISO model of active power. Nevertheless, studies that provide a steady controller configuration in an adaptive approach for both minor and major grid events, as well as a precise mathematical frequency analysis model for GFM APC and SGdynamics, are few. Consequently, the following contributions are made by this study: 1) The APC and simplified active power SISO model were used to perform stability study based on the SCR. The suggested technique increased the stability in both the Nyquist stability criteria and step response, and it was used to adaptively adjust the APC while considering SCR. 3) The time-domain simulation demonstrated the stability of an accurate mathematical-based SFR model that takes into account the suggested approach of a GFM APC. 4) The transient stability of both small and big grid events is improved by a suggested GFM APC that uses an adaptive technique for establishing parameters. This paper is organized and follows the following format: In II, the active-power SISO model is used to explain the APC arrangement. The stability issue in small-grid events is addressed in the third section, which presents the results of using a new controller. In IV, the outcomes of the simulations are compared and confirmed after a technique is given for mathematically interpreting the SFR model. The suggested approach is used to produce simulation results for large-grid events in V. Lastly, the results are detailed in

International Journal of Engineering Research and Science & Technology

ISSN 2319-5991 www.ijerst.com

Vol. 21, Issue 2, 2025

GFM INVERTER MODELING A. VOLTAGE-CONTROLLED PLANT MODEL

Fig. 1 shows the basic control structure of the voltage-source based GFMinverter. It contains a cascaded structure in which a current reference value is generated using the voltage control loop and a voltage reference value for pulse width

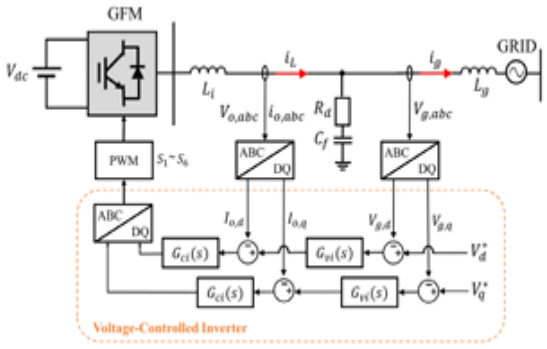

FIGURE 1. Structure of the voltage-controlled inverter control circuit. modulation (PWM)

Current control loops create switching. An LC-filter voltage source model is examined in this research, with GFM linked to the grid via the system impedance Zlv = ϋLgs+Rg. The formula for SCR, which is based on Lg per unit (p.u.), is SCR = 1/Zlv. Consequently, when the GFM is linked to the grid, SCR becomes a measure for assessing the PCC's resilience. Figure 2 shows the system that may be built using the control block diagram of the voltage-source-based GFM inverter (Fig. 1). The superposition concept is used to assemble Gclv(s) and Zov(s), the equivalent impedance of the inverter. Equation (1)~(7) describes the method of derivation for each transfer function. Gclv(s) is tasked with producing voltage after receiving the voltage reference V∏ o(s). The transfer function for the disturbance component of Vo(s) is formed by combining Zov(s) with the grid current ig(s) [24].

$$V_o(s) = G_{clv}(s)V_o^*(s) - Z_{ov}(s)i_g(s) \quad (1)$$

$$Y_{Li}(s) = \frac{1}{Z_{Lf}(s) + Z_{Cf}(s)} \quad (2)$$

$$G_{ii}(s) = \frac{Z_{Cf}(s)}{Z_{Lf}(s) + Z_{Cf}(s)} \quad (3)$$

$$G_{clv}(s) = \frac{T_v(s)}{1 + T_v(s)}, \qquad Z_{ov}(s) = \frac{Z_{oi}(s)}{1 + T_v(s)} \quad (4)$$

$$T_v(s) = \frac{G_{vi}(s)G_{ci}(s)G_{PWM}(s)Z_{Cf}(s)}{Z_{Lf}(s) + Z_{Cf}(s) + G_{ci}(s) * G_{PWM}(s)} \quad (5)$$

$$Z_{oi}(s) = \frac{Z_{Cf}(s)[Z_{Lf}(s) + G_{ci}(s) * G_{PWM}(s)]}{Z_{Lf}(s) + Z_{Cf}(s) + G_{ci}(s) * G_{PWM}(s)} \quad (6)$$

$$G_{vi}(s) = K_{vp} + \frac{K_{vi}}{s} \quad (7)$$

FIGURE 2. Block diagram of the voltage-controlled inverter. ZLf (s) and ZCf (s) represent the impedance of the fil ter inductor and a capacitor with a damping resistor.

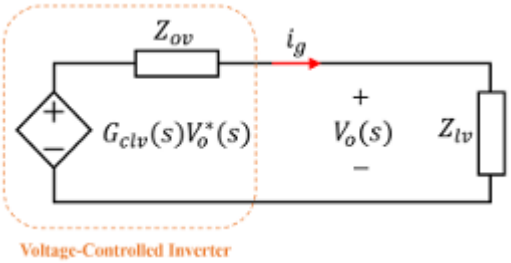

FIGURE 3. Impedance-based equivalent model for voltage-controlled inverter.

Gvi(s) denotes the voltage control loop's proportional-integral (PI) controller. Gci(s) is the controller for the proportional (P) current. It is presumed that GPWM(s) ≈ 1 because PWM has an adequately high switching frequency and almost little time delay. To review, the plant model was seen as a voltage transfer function in Eq. (1). Figuratively speaking, it's an impedance-based model that stands in for Eq. (1). Figure 3 shows that Gclv(s) controls GFM when it is acting as a voltage source. The inverter's equivalent impedance, Zov(s), and the grid's impedance, Zlv(s) = ϋLgs+Rg, are linked in

International Journal of Engineering Research and Science & Technology

ISSN 2319-5991 www.ijerst.com

Vol. 21, Issue 2, 2025

phase. The GFM-connected bus's SCR is denoted as Zlv(s), and the voltage reference determines the application of Vo(s). You may build V∏ o(s) according to Eq. (8) by using the inverter's equivalent impedance and the system SCR. Taking into account the GFM voltage control component and the system SCR, it is the GFM plant model's closed-loop transfer function [24].

$$\frac{V_o}{V_o^*(s)} = G_{clv}(s)\frac{1}{1+\frac{Z_{gi}(s)}{Z_{lv}(s)}} = G_v(s) \qquad (8)$$

GFM PLANT MODEL POLE CONSIDERING THE SCR

All of the settings used by the voltage-source based GFM are detailed in Table 1. An analysis was conducted on the plant model Gv(s) using the SCR. A transfer function without a PI controller Gvi was used to create the plant model for Eq. (8) in MATLAB. The pattern of the pole's change is seen when the SCR varies since the equation changes depending on the SCR. In Figure 4, we can see that when the SCR grows, the pole of Gv(s) shifts to the right part of the picture. According to the present value of the LC filter, the Gv(s) pole is in a stable state with a real axis value of −42∼−40. But this is only a feature of the plant model for GFM voltage; when active power is injected into the system, power stability analysis is required. This is due to the fact that both the grid system and GFM rely on voltage as their operating principle. Consequently, the instability of the system increases in relation to the proximity of the two voltage sources, or the greater the SCR, as the two sources exert mutual influences. When the SCRis low—that is, when the two voltage sources are physically far from one other—the system remains stable because the voltages produced by the sources are localized and have less impact on

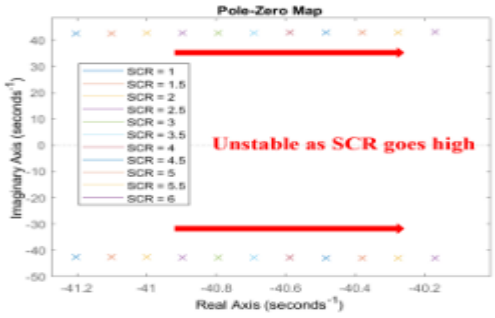

FIGURE 4. Grid-forming (GFM) inverter plant model pole considering the short-circuit ratio (SCR).

to one another. With an increase in SCR or changes to controller parameters, the voltage-source-based GFM with APC or other system circumstances might become unstable. Hence, it is necessary to do a stability study by taking into account the power characteristics of the GFM, including APC. This analysis will be covered in the next chapter.

POWER LOOP–ACTIVE POWER CONTROL (APC)

In order to conduct stability analysis based on frequency response, small-signal analysis is necessary. To do the math, we use a small-signal model of the grid-connected inverter's injected active and reactive power into the system. Incorporating an external control loop into Gv(s) yields the active power output. A reactive power control (RPC) that regulates the voltage in a manner similar to that of a synchronous generator and an angle-controlling APC make up the outer control loop. The APC section allows for the configuration of a droop control that mimics the governor's droop and a VSM that can model the generator's swing equation and damping. The RPC uses Q-droop control to create the voltage reference value. Nonetheless, the SISO model's stability analysis of active power remains the main emphasis. Furthermore, it is assumed that V∗ o(s) = Vo(s) = 1 p.u. since there is a modest voltage response caused by small changes in the active power when robust control settings are used. Obtaining the small-signal models of the GFM's active and reactive power components is important to create a GFM power loop based on the SISO model. This is how the active and reactive powers' outputs are described [25]:

International Journal of Engineering Research and Science & Technology

ISSN 2319-5991 www.ijerst.com

Vol. 21, Issue 2, 2025

$$P = \frac{3V_o[(V_o - V_g\cos\delta_0)R_g + V_gX_g\sin\delta_0]}{2(R_g^2 + X_g^2)} \quad (9$$

$$Q = \frac{3V_o[(V_o - V_g\cos\delta_0)X_g - V_gR_g\sin\delta_0]}{2(R_g^2 + X_g^2)} \quad (10$$

$$P = K_{p\delta}\hat{\delta} + K_{pv}\hat{V}_0$$
$$\hat{Q} = K_{q\delta}\hat{\delta} + K_{qv}\hat{V}_0 \quad (11)$$

Typically, KpŬ and Kqv are the sole variables examined in this work since P is the major variable in angle and Q is the main variable in voltage. Here are the formulas for Kpδ and Kqv:

$$K_{p\delta} = \frac{3V_oV_g(R_g\sin\delta_0 + X_g\cos\delta_0)}{2(R_g^2 + X_g^2)}$$
$$K_{qv} = \frac{3V_o(2V_oX_g + V_g(-R_g\sin\delta_0 - X_g\cos\delta_0))}{2(R_g^2 + X_g^2)} \quad (1$$

$$G_p(s) = \frac{\theta_{o,ref}(s)}{P_{ref}(s) - P_{meas}(s)} = \frac{\omega_oR_p}{s}$$
$$G_q(s) = \frac{V_{o,ref}(s)}{Q_{ref}(s) - Q_{meas}(s)} = V_oR_q \quad (15)$$

The SISO model is simplified by assuming that the sole relational expression associated to the active power measurement Pmeas of the GFM is Kpδ, where δ is the active power. The open-loop transfer function (OLTF) of reactive power is left out of the stability analysis of the active power output equation since it assumes that the voltage is 1 p.u. Figure 5 shows the OLTF of active power, which is shown below:

$$G_{p\_open}(s) = G_p(s)G_v(s)K_{p\delta} \quad (16)$$

If the initial GFM is integrated and synced with the system, and Xg > Rg in Kpδ, then there is no phase angle difference between the two. So, δ0 is equal to zero.. The active power's final simplified OLTF is equal to Equation (17).

PROPOSED CONTROL

DIFFERENTIATOR WITH SCR DAMPING (DTSD)

According to the SCR, the GFM plant model started to become unstable. It suggests that if the GFM APC does not adequately adjust for the unstable component based on the SCR, the active power SISO model can also be unstable. Previous studies have shown that with high SCR, droop sensitivity and damping must be tuned to substantial values [18]. Consequently, getting

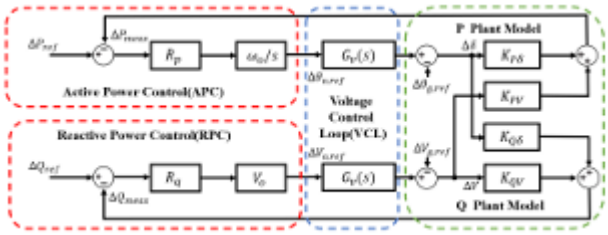

FIGURE5. APCopen-looptransferfunction(OLTF).

TABLE1. Parametersandvariabledefinitions.

Symbol	Name	Value
S_n	Rated capacity	100 MVA
V_g	Rated grid voltage	22.9 kV
ω_o	Fundamental angular frequency	377 rad/s
X_g/R_g	Grid-side impedance X/R ratio	1
L_i	Inverter-side inductance	0.2 mH
C_f	Filter capacitance	20 μF
R_d	Passive damping resistance	0.5 Ω
K_{vi}	Integral gain of voltage controller	25
K_{vp}	Proportional gain of voltage controller	1
K_{cp}	Proportional gain of current controller	1
R_p	Droop control constant	0.05
H_{vsm}	VSM inertia constant	1
D_{vsm}	VSM damping constant	40
T_1	DTSD delay	5.0
α	DTSD alpha	0.8
β	DTSD beta	0.8

adaptively set droop and damping with respect to SCR. The parameters were established using an

International Journal of Engineering Research and Science & Technology

ISSN 2319-5991 www.ijerst.com

Vol. 21, Issue 2, 2025

exponential function form, which varied throughout many SCR ranges. The usage of arbitrary exponential functions was suggested to be prevented by proposing an exponential function with a basis, which indicates optimal parameter choices for different SCRs. This research suggests a differentiator with SCR damping (DTSD) controller that takes SCR into account in the exponential function, as a high SCR might cause unstable features in the present droop and VSM controllers. This is the control block diagram of the DTSD. The dampening step involves quantifying the SCR and applying the GFM to the controller. By dynamically changing α and β depending on the SCR, the GFM may determine the droop or damping sensitivity. Then, as indicated in Figure 6, the differentiator component was made up of the droop and VSM with a differentiator time delay V1. You may succinctly describe DTSD as OLTFas seen in equation (17), and it also comprises the APC of the GFM. The following is the Gp(s) of droop, including DTSDisas, while Gv(s) stays the same:

$$G_p(s) = \frac{\omega_o}{s}\frac{R_p}{(1+\alpha e^{\beta SCR}R_p)}(1+\frac{sT_1}{1+sT_1}) \quad ($$

$G_p(s)$ of VSM including DTSD is as follows.

$$G_p(s) = \frac{\omega_o}{s}\frac{1}{2H_{vsm}s + D_{vsm} + \alpha e^{\beta SCR}}(1+\frac{sT_1}{1+sT_1}) \quad ($$

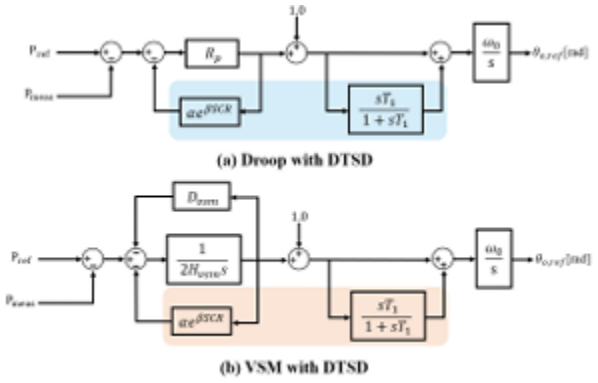

FIGURE6. ProposeddifferentiatorwithSCRdamping(DTSD)controller.

The control block is a two-parameter natural exponential function that gives feedback in the droop or inertia component. α, a parameter that determines the degree of effect of the damping, allows GFM to change the sensitivity of the overall DTSD controller. Further dampening of the angle might enhance the sensitivity if it is set to a high degree. The dependency on SCR may be adjusted by the GFM in the case of β. For large settings, it is possible to replicate the dynamic properties of different SCRs. By cautiously adjusting the parameters based on the SCR, the output change may be made to be minimal if β is modest. At last, the controller is finished by connecting the differentiator to produce the angle, and it is adaptively programmed by establishing the SCR as a variable. B, α and β are assigned to values between 0 and 1.

STABILITYACCORDINGTODTSDPARAMETERS

The Nyquist diagram result of Eq. (17) was utilized for APC, as shown in Fig. 6, and it is based on GFM values mentioned in Table 1. The SCR was adjusted to a high value of 6 in order to compare findings in terms of α, while β was fixed at 0.5. The sensitivity of the damping value depending on SCR causes the droop to migrate to the stable region in the Nyquist diagram as α grows. For values of α that are 0.2, 0.5, and 0.8. To rephrase, more enhancement is necessary for steady functioning since the current dosage is inadequate.

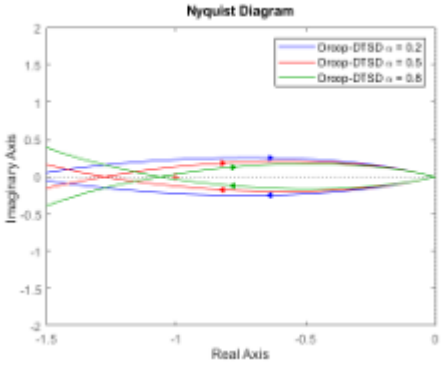

FIGURE7. NyquistplotaccordingtoαofDroop-DTSDwhenSCR=6and β=0.5.

International Journal of Engineering Research and Science & Technology

ISSN 2319-5991 www.ijerst.com

Vol. 21, Issue 2, 2025

SYSTEM FREQUENCY RESPONSE MODELING

SYSTEM FREQUENCY RESPONSE MODELING WITH DROOP, VSM, AND DTSD

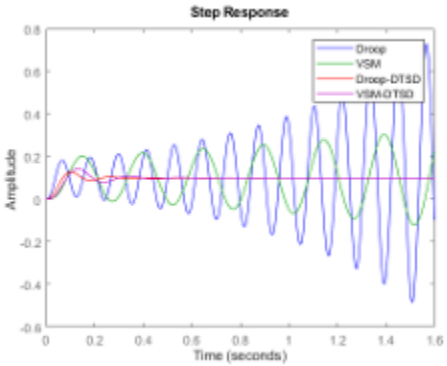

FIGURE 13. Step response compared with droop, VSM, and DTSD in high-SCR cases.

it is also important to study the power for frequency response in big grid events. This is due to the fact that GFM's frequency responses are articulated as an additional mathematical model that relies on the arrangements of the power system, including governor and inertia in big grid events. Furthermore, the GFM power could differ depending on the GFM's APCcontrol settings [17], [18]. So, this section takes the SFR model and applies it quantitatively using the swing equation that is based on the SG's mechanical properties [32]. The SFR model will also include the steps need to execute the different APC controls of GFM. A study was carried out in the SFR model with a single generator capable of simulating the same system and GFM with APCcontrollers. In the simplified SFR model study, the generator's damping parameters and headroom were disregarded. The frequency response was enhanced by the use of Pd as a step response. To set the governor's parameters, we use average values taken from thermal power plants [32]. The process of frequency production is provided by Eq. (20)~(22), where s is the Laplace derivative term, because the generator and GFM use the swing equation to produce frequencies. Here is the formula for frequency generation of an SG that does not take dampening into account:

$$\frac{d\theta_o}{dt} = \omega_o = R_p \Delta P \qquad (21)$$

$$\frac{d\theta_o}{dt} = \omega_o = \frac{1}{2H_{vsm}s + D_{vsm}} \Delta P \qquad (22)$$

The governor of the generator feeds back ü in order to produce mechanical power Pm, and the frequency's dynamic condition is always changing. In a synchronized area, when the generator and GFM are coupled, üg = üo = ü.

$$\frac{d^2\theta_g}{dt^2} = s\frac{d\theta_g}{dt} = s\omega_g = \frac{\Delta P}{2H}, \Delta\omega_g = \frac{\Delta P}{2Hs} \qquad (20)$$

International Journal of Engineering Research and Science & Technology

ISSN 2319-5991 www.ijerst.com

Vol. 21, Issue 2, 2025

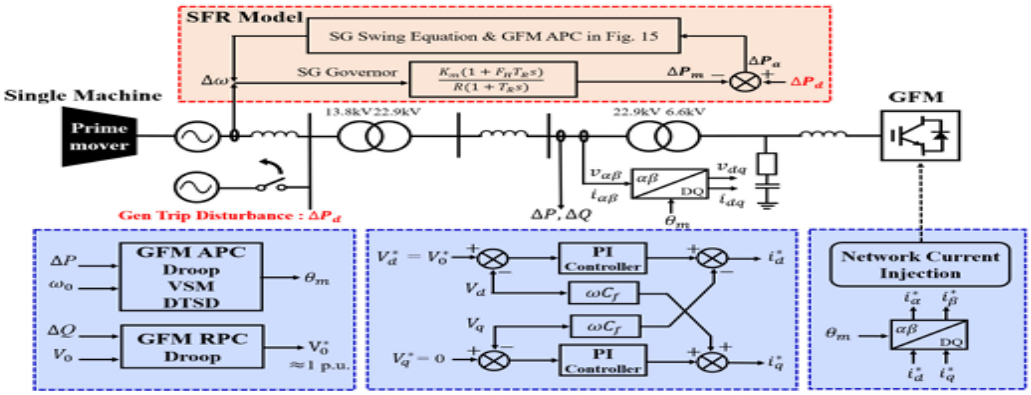

FIGURE14. EquivalentsystemstructurecomprisingageneratorwithgovernorandGFM

.

Thus, Fig. 15 displays the expressions of υ and PdinSFR that represent the process. According to the frequency-formation-formula-of-droop using DTSD,

$$\frac{d\theta_o}{dt} = \omega_o = \frac{R_p}{1+\alpha e^{\beta SCR} R_p}\left(1+\frac{sT_1}{1+sT_1}\right)\Delta P \qquad (23)$$

$$\frac{d\theta_o}{dt} = \omega_o = \frac{1}{2H_{vsm}s + D_{vsm} + \alpha e^{\beta SCR}}\left(1+\frac{sT_1}{1+sT_1}\right)\Delta$$

SFR MODELVALIDATION

The SG and governor parameters used in the SFR model are summarized in Table 2. Table 1 lists the remaining PI controller gains, filter settings, and DTSD parameters. A dynamic model capable of simulating GFM does not exist in the time-domain simulation PSS/e used in this investigation. Hence, a controller consisting of an APC, RPC, and voltage control loop was modeled using a user-defined model (UDM) based on numerical integration. This GFMUDM model was then incorporated into a PSS/e system to simulate large-gride events. The resulting structure is depicted in Figure 14. Proven in a test system, the findings showcase the enhanced performance of the suggested technique. Figure 14 shows the test system, which includes GFMs and SGs with a governor that can replicate the system equivalently. Each power production source is set to 100MVA. According to Figure 16, the MATLAB nadir frequency is 59.785 Hz in 1.5 seconds, the Pss/e ratio is 59.7854 Hz in 1.57 seconds, and both graphs converge to 59.83 Hz for the drop. The frequency observed using MATLAB was 59.873 Hz in the example of VSM depicted in Fig. 16.

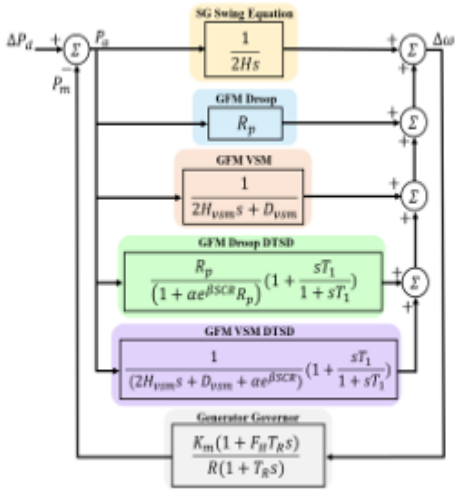

FIGURE15. Systemfrequencyresponse(SFR)model, includingdroop, VSM,andDTSD.

TABLE2. SFRmodelparametersandsimulations.

International Journal of Engineering Research and Science & Technology

ISSN 2319-5991 www.ijerst.com

Vol. 21, Issue 2, 2025

Symbol	Name	Value
H	Generator inertia	5
R	Governor droop	0.05
K_m	Mechanical power gain factor	1
F_H	Fraction of total power generated by the HP turbine	0.3
T_R	Reheat time constant, s	8.0
ΔP_d	Load step magnitude	0.1

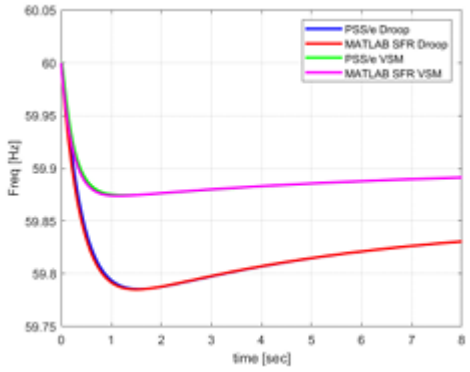

FIGURE 16. Validation of MATLAB SFR model and PSS/e simulation results.

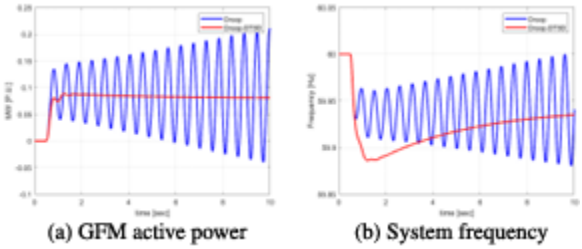

FIGURE 17. Droop and droop with DTSD results in low-droop case.

fully accurate. At last, we can extract these two significant outcomes. 1) The GFM transfer function proves a number of APC controls. 2) The frequency response and scenario of major grid occurrences may be analyzed using the GFM UDM in PSS/e. Section V: Model Outcomes This part analyzes the performance of the proposed technique against the system and offers the simulation results to contrast with the real divergence situations, as illustrated in Figure 14. The model was run with the following parameters: SG and GFM each had 100 MVA, and the generator trip was 10 MW, or 10% of the base capacity. Table 1 provides the basis for the GFM control parameters, whereas Table 2 provides the basis for the SG governor settings. A. Cases with an unstable low-drop As seen in Figure 17, droop was carefully adjusted by SCR damping with α and β according to Table 1 in order to mimic unstable output scenarios in droop. It was assumed that SCR was 6, and droop was adjusted from 0.05 to 0.0117. In PSS/e time-domain simulation, the sensitive droop value is compared both with and without a differentiator. Figure 17(a) shows that in the absence of a differentiator, droop causes the active power to diverge. Nevertheless, a differential DTSD component injection will fix this issue. While the active power remains constant in droop with DTSD, the sensitivity of droop is adjusted and a differentiator is added into the controller. Reason being, droop in conjunction with a differentiator guarantees stable active power and decreases overshoot in

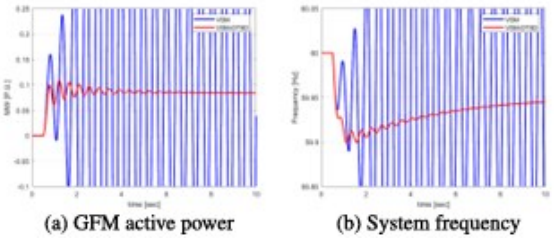

FIGURE 18. VSM and VSM with DTSD results in the high-damping case.

substantial grid-based events. Finally, droop with differentiator outputs converge to 8.1 MW, or 0.081 p.u., and may reach 8.8 MW, or 0.088 p.u. It seems that overshoot happens over 10 MW in the scenario when just droop is present, but it keeps diverging after that. Figure 17(b) displays the frequency findings derived from the GFM's active power. The rated capacity of GFM and SG in the test system was 100 MVA. The system's active power supply and demand will likewise become unstable if GFM injects unstable active power. Consequently, the test system is very sensitive to the GFM's output. Figure 17 shows that the frequency likewise diverges without stabilizing when the GFM diverges. System frequency fluctuations are also stable since the DTSD droop injects active power consistently. A nadir frequency of 59.886 Hz is recorded by droop with differentiator, which converges to 59.94 Hz, in

International Journal of Engineering Research and Science & Technology

ISSN 2319-5991 www.ijerst.com

Vol. 21, Issue 2, 2025

contrast to droop without differentiator, which causes the system frequency to collapse. It is crucial to prevent power divergence instability of GFM by performing droop controller design considering the differentiator, as demonstrated in the findings.

UNSTABLE VSM CASES WITH HIGH DAMPING

The unstable output VSM situation was analyzed via simulation in this subsection. In the event that the active power-sensitive damping value of the VSM, Dvsm, is set to a high value, the integrator's output that is dependent on the VSM inertia may not be appropriately connected to the parameters of the voltage control loop, and it may diverge. Hence, Dvsm is adjusted between 40 and 105.16 according to α and β in Table 1, and SCR is presumed to be 6. Using the same simulation settings as droop, we compared the outcomes with and without differentiator. Figure 18(a) shows that the VSM damping is sensitively tuned; nonetheless, the output diverges in the absence of a differentiator. The results of VSM with a differentiator show no significant change. Even with a sensitive damping value increase, the differentiator considerably improves overshoot performance, much like in the prior droop instance. Here, VSM with differentiator peaks at 11.0 MW (or 0.11 p.u.) and fades to 8.4 MW (or 0.084 p.u.). Without a differentiator, it first diverges after over 15 MW. The Hvsm component causes a temporal delay in the APC in VSM, unlike droop, which means that bigger oscillations are possible. As a result, the output could become unstable if Hvsm is set too high since the time delay grows and additional time delay filtering is done. Hence, a sufficiently low value for Hvsm is required. As seen in Figure 18(b), if the VSM output is not steady, the system frequency will also diverge. A differentiator-based VSM converges to 59.95 Hz after reaching a nadir frequency of 59.9 Hz. However, the system frequency likewise collapses when VSM is not used with a differentiator. Using the differentiator, the output may be kept stable even in the situation of VSM if the damping value is set to a very high value or if the damping is enhanced by the α and β of the suggested DTSD.

Conclusion

To stabilize the system, this work built an active power OLTF transfer function with APC based on the SISO model and used the suggested approach that is based on the SCR. Nyquist stability analysis and step responses demonstrated that the DTSD shown in the small-grid event outperformed the current droop and VSM. With the use of SFR modeling in large-grid events, the DTSD, VSM, and droop controllers were also mathematically modeled. This investigation confirmed that the transfer function based on different APC was correctly set by comparing the results of the MATLAB and PSS/e simulations. Then, even with the most delicate droop and VSM parameter adjustments, the suggested DTSD ensured a steady output. Applying the suggested approach in conjunction with a GFM would therefore resolve stability issues during minor grid events and guarantee a reliable output during big grid events. The frequency response should be achieved by thorough SFR, which includes all IBRs with other frequency control, and adaptive parameter setting based on the varied capabilities of GFM should be examined in subsequent study.

REFERENCES

[1]. L. Huang, C. Wu, D. Zhou, and F. Blaabjerg, ‘‘A double-PLLs-based impedance reshaping method for extending stability range of grid following inverter under weak grid,’’ IEEE Trans. Power Electron., vol. 37, no. 4, pp. 4091–4104, Apr. 2022.

[2]. X. Zhang, D. Xia, Z. Fu, G. Wang, and D. Xu, ‘‘An improved feedforward control method considering PLL dynamics to improve weak grid stability of grid-connected inverters,’’ IEEE Trans. Ind. Appl., vol. 54, no. 5, pp. 5143–5151, Sep. 2018.

[3]. Q. Hu, R. Han, X. Quan, Z. Wu, C. Tang, W. Li, and W. Wang, ‘‘Grid-forming inverter enabled virtual power plants with inertia support capability,’’ IEEE Trans. Smart Grid, vol. 13, no. 5, pp. 4134–4143, Sep. 2022.

[4]. Y.Lin,J. H.Eto, B.B.Johnson,J. D.Flicker, R. H. Lasseter, H. N. V. Pico, G.-S. Seo, B. J. Pierre, and A. Ellis, ‘‘Research roadmap on grid forming inverters,’’ Nat. Renew. Energy Lab. (NREL), Golden, CO, USA, Tech. Rep. NREL/TP-5D00-73476, 2020.

[5]. J. Liu, Y. Miura, and T. Ise, ‘‘Comparison of dynamic characteristics between virtual synchronous generator and droop control in inverter-based distributed generators,’’ IEEE Trans. Power Electron., vol. 31, no. 5, pp. 3600–3611, May 2016.

[6]. J. Song, M. Cheah-Mane, E. Prieto-Araujo, and O. Gomis-Bellmunt, ‘‘Short-circuit analysis of AC distribution systems dominated by voltage source converters considering converter limitations,’’ IEEE Trans. Smart Grid, vol. 13, no. 5, pp. 3867–3878, Sep. 2022.

[7]. W. Wu, Y. Chen, A. Luo, L. Zhou, X. Zhou, L. Yang, Y. Dong, and J. M. Guerrero, ‘‘A virtual inertia control strategy for DC microgrids analogized with virtual synchronous machines,’’ IEEE Trans. Ind. Electron., vol. 64, no. 7, pp. 6005–6016, Jul. 2017.

International Journal of Engineering Research and Science & Technology

ISSN 2319-5991 www.ijerst.com

Vol. 21, Issue 2, 2025

[8]. S. D'Arco and J. A. Suul, ''Equivalence of virtual synchronous machines and frequency-droops for converter-based MicroGrids,'' IEEE Trans. Smart Grid, vol. 5, no. 1, pp. 394–395, Jan. 2014.

[9]. M. Chen, D. Zhou, A. Tayyebi, E. Prieto-Araujo, F. Dörfler, and F. Blaabjerg, ''Generalized multivariable grid-forming control design for powerconverters,'' IEEE Trans. Smart Grid, vol. 13, no. 4, pp. 2873–2885, Jul. 2022.

[10]. B. B. Johnson, S. V. Dhople, A. O. Hamadeh, and P. T. Krein, ''Synchronization of nonlinear oscillators in an LTI electrical power network,'' IEEE Trans. Circuits Syst. I, Reg. Papers, vol. 61, no. 3, pp. 834–844, Mar. 2014.

[11]. M. Lu, ''Virtual oscillator grid-forming inverters: State of the art, modeling, and stability,'' IEEE Trans. Power Electron., vol. 37, no. 10, pp. 11579–11591, Oct. 2022.

[12]. Grid Forming Technology Bulk Power System Reliability Considerations, NERC, North American Electric Reliability Corporation, Atlanta, GA, USA, 2021.

[13]. AEMO, Voluntary Specification for Grid-Forming Inverters, Australian Energy Market Operator (AEMO), Melbourne, VIC, Australia, May 2023.

[14]. L. Zhang, L. Harnefors, and H.-P. Nee, ''Power-synchronization control of grid-connected voltage-source converters,'' IEEE Trans. Power Syst., vol. 25, no. 2, pp. 809–820, May 2010.

[15]. R. Rosso, J. Cassoli, G. Buticchi, S. Engelken, and M. Liserre, ''Robust stability analysis of LCL filter based synchronverter under different grid conditions,'' IEEE Trans. Power Electron., vol. 34, no. 6, pp. 5842–5853, Jun. 2019.

[16]. X. Wang, M. G. Taul, H. Wu, Y. Liao, F. Blaabjerg, and L. Harne fors, ''Grid-synchronization stability of converter-based resources—An overview,'' IEEE Open J. Ind. Appl., vol. 1, pp. 115–134, 2020.

[17]. T. Qoria, E. Rokrok, A. Bruyere, B. François, and X. Guillaud, ''A PLL-free grid-forming control with decoupled functionalities for high-power transmission system applications,'' IEEE Access, vol. 8, pp. 197363–197378, 2020.

[18]. Y. Mitsugi and J. Baba, ''Phaser-based transfer function analysis of power synchronization control instability for a grid forming inverter in a stiff grid,'' IEEE Access, vol. 11, pp. 42146–42159, 2023.

[19]. P. C. Loh and D. G. Holmes, ''Analysis of multiloop control strategies for LC/CL/LCL-filtered voltage-source and current-source inverters,'' IEEE Trans. Ind. Appl., vol. 41, no. 2, pp. 644–654, Apr. 2005.